LOW RESISTIVITY PAY DEVELOPMENT: CASE STUDY OF TALANGAKAR FORMATION ASRI BASIN, OFFSHORE SOUTHEAST SUMATRA, INDONESIA

PENGEMBANGAN INTERVAL RESISTIVITAS RENDAH: STUDI KASUS FORMASI TALANGAKAR CEKUNGAN ASRI, LEPASPANTAI SUMATRA TENGGARA, INDONESIA

Dwandari Ralanarko[1*], Pranowo Nugroho[1], Edy Sunardi[2], Ildrem Syafri[2] and Billy G. Adhiperdana[2]

[1] Pertamina Hulu Energi OSES, Menara Standard Chartered, Jl. Prof. Dr. Satrio No.26, Karet Semanggi, Setiabudi, Jakarta Selatan, DKI Jakarta 12950

[2] Post-Graduate Program, Faculty of Geological Engineering – Universitas Padjadjaran, Jl. Raya Bandung – Sumedang KM 21, Jatinangor, Jawa Barat 45363

*Corresponding author: dwandari.ralanarko@gmail.com

(Received 23 January 2023; in revised from 24 January 2023; accepted 14 April 2023)

DOI : 10.32693/bomg.38.1.2023.803

ABSTRACT: Southeast Sumatra is a prolific oil and gas block located offshore in the Java Sea, 90 km north of Jakarta Bay. This area covers two major basins, namely Sunda Basin and Asri Basin. The initial development of the area focused on faulted and high closures and high-resistivity reservoirs. Further analysis shows that there are special low-resistivity reservoirs in Widuri Area, especially in the Aryani field. This paper will discuss the low resistivity pay zone reservoirs and fluid containment of the intervals. The paper will also include further assesment this undeveloped interval to increase oil production, considering the upside potential of the reservoirs using current geological, geophysical, and reservoir engineering approaches. Additionally, it will describe the operational challenges faced during the production period.

The low-resistivity pay zone, a hydrocarbon-bearing reservoir in the Aryani field of the Widuri area, was identified using gas readings in the daily drilling reports, complemented with mud logging data. The Basal Sand interval, which drapes above the basement, was the site of the first producing well of Basal Sand, Aryani AC-X, preceded by a hydraulic fracturing job. Lambda-mu-rho inversion was implemented to delineate this reservoir. To recognize the potency in those wells, data reconfirmation was conducted between the elan summary, sidewall core, and cutting data. Aryani AC-X has successfully drained oil using a submersible pump, with an initial production of 408 bopd and cumulative production of 240 MBO.

Keywords: Asri Basin, Indonesia, low resistivity, Oligo-Miocene, reservoir, Talangakar Formation

ABSTRAK: *Southeast Sumatra merupakan blok minyak dan gas yang produktif yang terletak di lepas pantai Laut Jawa sekitar 90 km sebelah Utara Teluk Jakarta. Daerah ini mencakup dua cekungan utama, yaitu Cekungan Sunda dan Cekungan Asri. Pengembangan awal area ini difokuskan pada lokasi yang memiliki konfigurasi struktur tinggian dan reservoir dengan resistivitas tinggi saja. Analisis lebih lanjut menunjukkan bahwa terdapat reservoir tertentu yang memiliki resistivitas rendah di Cekungan Asri, terutama lapangan Aryani. Makalah ini akan membahas tentang identifikasi reservoir resistivitas rendah dan jenis fluida hidrokarbon yang terakumulasi. Makalah ini juga membahas kelakuan reservoir menggunakan pendekatan geologi, geofisika, dan teknik reservoir, serta menjelaskan tantangan operasional produksi.*

Zona hidrokarbon dengan resistivitas rendah di Lapangan Aryani Cekungan Asri diidentifikasi menggunakan pembacaan gas pada laporan pemboran harian yang dilengkapi dengan data mud logging. Interval Basal Sand yang membentang diatas basement merupakan site sumur produksi pertama dari Basal Sand, yaitu sumur Aryani AC-X, yang didahului dengan pekerjaan rekah hidrolik sebelum produksi. Inversi Lambda-Mu-Rho diimplementasikan untuk mendelineasi reservoir ini. Rekonfirmasi data antara Elan Summary, Sidewall Core dan Cutting dilakukan untuk mengetahui potensi di sumur tersebut. Aryani AC-X telah berhasil mengalirkan minyak dengan menggunakan pompa submersible, dengan produksi awal 408 bopd dan produksi kumulatif tidak kurang dari 240 MBO.

INTRODUCTION

Southeast Sumatra Production Sharing Contract is located in Offshore Southeast Sumatra, operated by Pertamina Hulu Energi OSES. Three basins of Sunda, Asri, and Hera lie in an area of 11,046 sq. km of concession. Asri Basin was once thought to have low maturity of source rocks resulting in a low interest to be explored, during the early stage, from 1983 to 1987 (Wight et al., 1997).

A Cenozoic extensional back-arc and half-graben rift of Asri Basin (Young and Atkinson, 1993) is situated in Offshore Sumatra, Indonesia, and covers an area of approximately 3500 sq. km. It comprises thick sediment from Paleocene to Pleistocene up to 16,000 ft in thickness. The basin is bordered by a downthrown to the west, N-S trending faults to the East, and an NW-SE trending wrench system to the south (Ralanarko et al., 2020).

Three major tectonics are recognized: pre-rift, syn-rift, and post-rift, which affected the structural style and depositional systems in the Asri Basin (Ralanarko et al., 2020). Stratigraphy of the Asri Basin is influenced by moderate intra-basinal faulting and folding. Structural control on major axial drainage systems would exert tremendous influence on sand supply to any particular basin at any given time. Basin integration and the control of axial fluvial systems play an important role in fluvial deposition during basin evolution and fill. The Lower Zelda and Upper Gita Members are the main components of the Oligocene Talangakar Formation (Aldrich et al., 1995). Figure 1a shows the location of the Asri Basin, while Figure 1b illustrates the regional stratigraphy.

The main objective of this research is early syn-rift Basal Sand interval, especially in the Aryani field. The reservoir is located above the basement fault and has a distinctive character, with a thickness of about 10 ft. This interval reservoirs in the area differ from other Talangakar Formation (TAF), in which sand was deposited by a meandering river system that streamed from the northwest to the southeast within the basin (Ralanarko et al., 2021).

Resistivity log patterns in this interval appear relatively flat and do not show any contrast with the layer above. However, the density log indicates a strong contrast with the layer above. The difference in trends between the two logs is assumed to be attributed to the presence of certain minerals that affect the resistivity log readings. Several minerals that can affect resistivity log readings

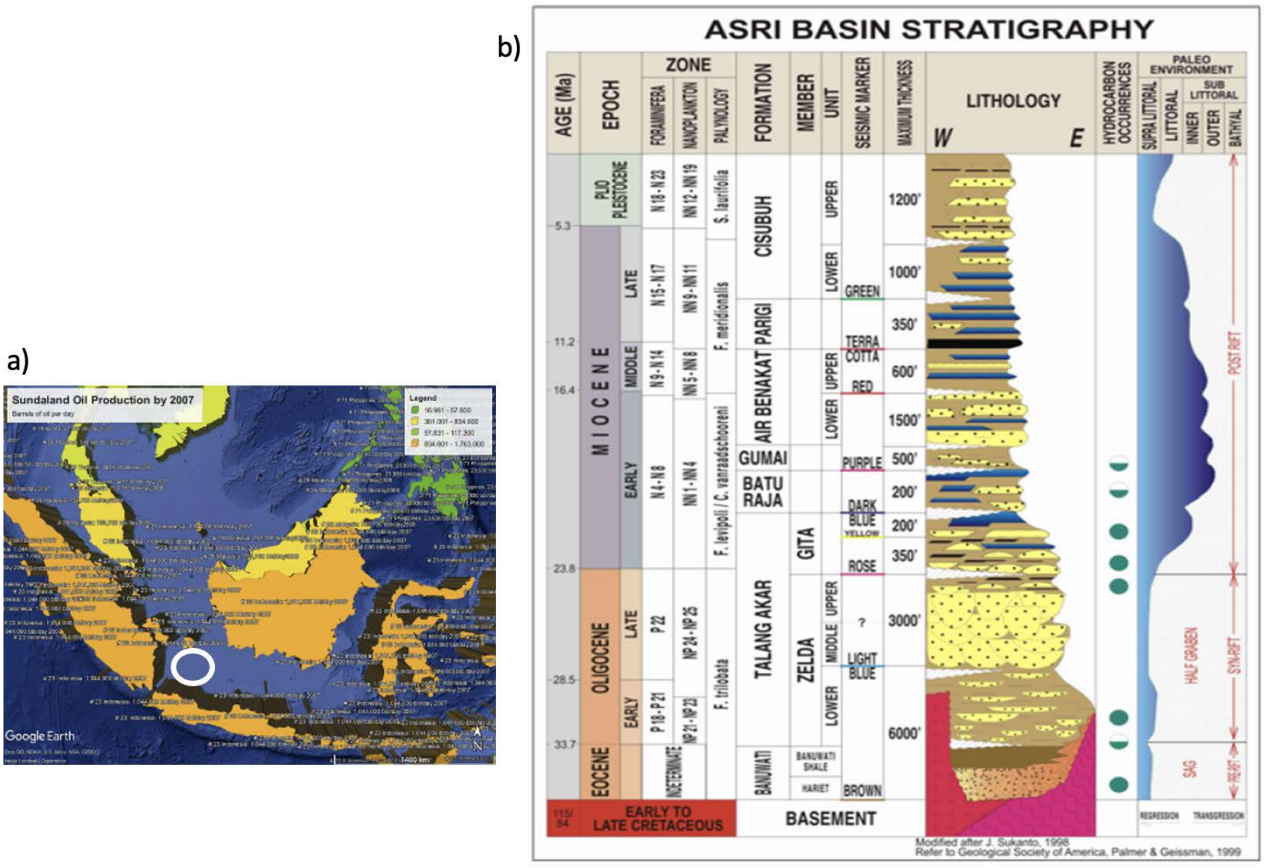

Figure 1.Asri basin location inside circle (a) and regional stratigraphy (b) (Ralanarko et al., 2020)

including clay minerals, such as clay minerals with high surface area and high cation exchange capacity, can impact the conductivity of the formation. As a result, lower resistivity readings may be observed on the resistivity log.

METHODS

The Basal Sand reservoir in the Aryani field has produced about 215 MBO from the A-05 well since it was first drilled in 2007. Based on the newest palaeogeography reconstruction conducted in this area, this interval are deposited earlier compare to the main reservoir interval in Talangakar Formation which was deposited in Upper Zelda and Gita interval (Ralanarko et al., 2021). Since only one well is currently producing from the reservoir and the average permeability is relatively low to medium, additional infill wells are needed to optimize production. The addition of well/infill drilling requires integrated reservoir characterization.

The study includes integrated geological modelling with seismic attributes to determine the lateral distribution of the Basal Sand reservoir. Vertical distribution-specific methods are needed because the Volume of Clay (VCL) and Gamma Ray (GR) logs alone are insufficient to separate thin layers in detail (Aki and Richards, 1980). In this study, we distinguished the reservoir characteristics and quality using Rock Typing (RT) methods. RT methods are used to classify an interval with similar characteristics in a particular zone (Smith and Gidlow, 1987). This process involves Cluster Analysis, which is based on statistical algorithms that classify image logs (FMI) and triple combo well logs data consisting of Gamma Ray, Neutron-Density and Resistivity that show similar characteristics. The zones along the wells were then determined based on grain size, grain shape, and sorting characteristics obtained from core data.

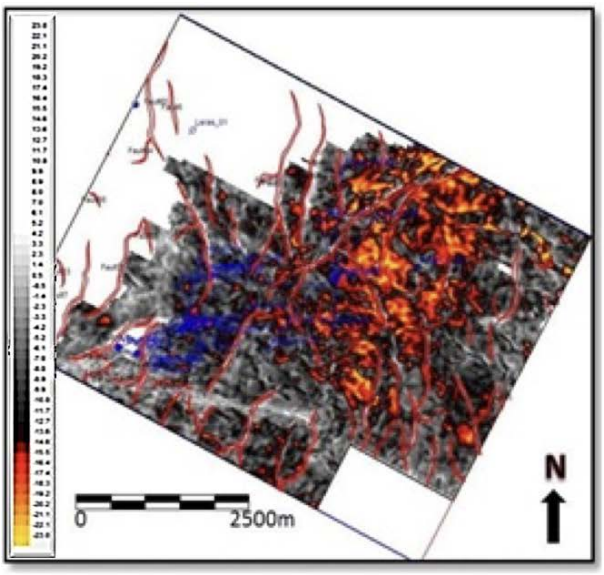

Figure 2a. Minimum amplitude attributes

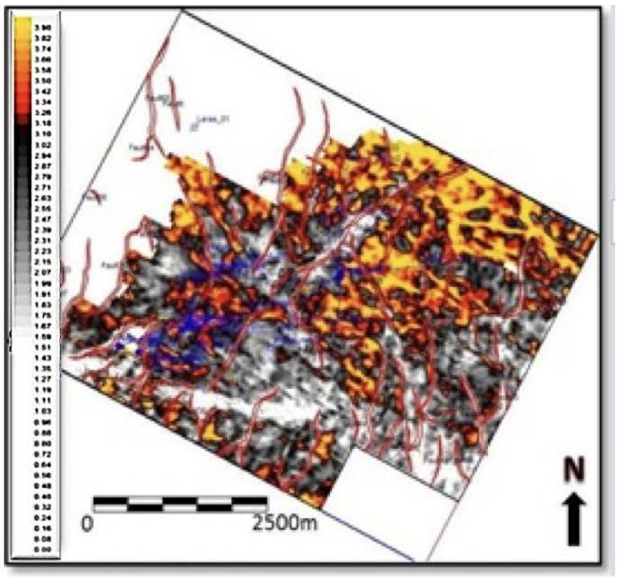

Figure 2b. Sweetness amplitude attribute

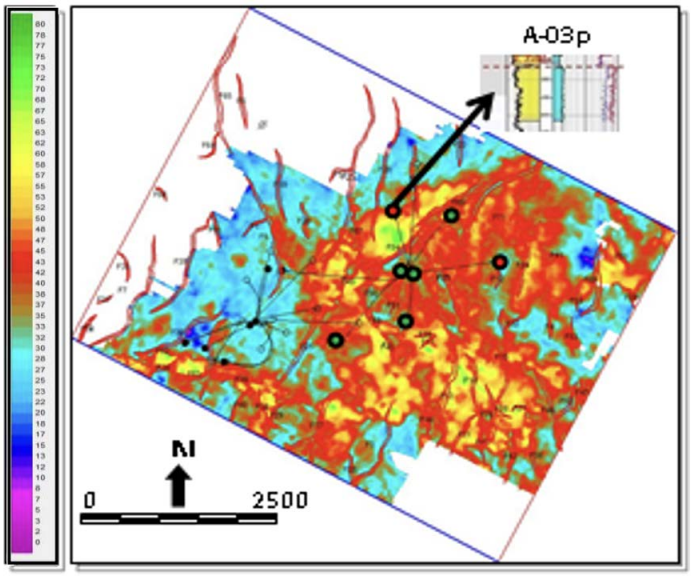

Figure 3. Isochrones interval Top Lower Zelda to the Top Basement

Geophysical Aspect

The Basal Sand is represented by a peak amplitude (a positive value indicates increased impedance) that interferes with the basement reflector. Amplitude attribute analysis was performed to determine the amplitude response of the Basal Sand. The minimum and sweetness amplitude attributes are shown in Figure 2a and Figure 2b. Unfortunately, the results were not sufficient to determine the lateral distribution of the Basal Sand.

After crosschecking with the presence of Basal Sand, many inconsistencies cannot be interpreted from the amplitude attributes. The common interpretation for predicting this Basal Sand is using isochrones from the Top Lower Zelda to the Top Basement as shown in Figure 3. These isochrones are

interpreted as the paleo-structures, especially regarding the distribution of the Basal Sand that drapes above the basement, thus controlling the depositional periods for the Lower Zelda member.

From this interpretation, the boundary of the lower Zelda member geometry has an NW–SE trend but for the Basal Sand distribution still an inconsistency between the well log and core data with the isochrones maps. An integrated geophysical analysis is needed for Basal Sand reservoir characterization.

Geological Aspect

In this case study, two commonly used Rock Typing (RT) methods, the flow-zone indicator (RQI/FZI) and the pore-throat radius (Winland's R (35)), have been applied (Guo et al., 2007). Both methods are applied to this case study.

The flow-zone indicator (RQI/FZI) method is a technique that uses the relationship between the rock quality index (RQI) and the formation factor indicator (FZI) to classify rocks into different types or zones based on their pore size distribution and permeability. The RQI measures the rock's strength and hardness, while the FZI measures of the porosity and permeability. This method is useful for identifying different flow zones within a reservoir.

The Winland's R (35) method is a technique that calculates the ratio of the volume of clay and other fine-grained minerals to the volume of pore space within a rock sample. This method is useful for determining the dominant pore-throat size and the permeability of the rock. A low Winland's R (35) value indicates that the rock has a high proportion of clay and fine-grained minerals, which can result in low permeability.

Both methods can provide valuable information about the characteristics of the rock formation, and can be used to help optimize oil and gas production. Based on the test results, the RQI/FZI is more in line with the Aryani field data. This is possible because the characteristics of clastic reservoirs in the Aryani field are most likely influenced by the texture, so permeability should correlate well with porosity.

Permeability is obtained from core data and distributed to the uncored well using the equation derived from the porosity and permeability cross plot. The ratio of RQI/FZI can be used to calculate rock typing (Amaefule et al., 1993). RQI is a rock-quality index given by:

$$RQI = 0.0314 \sqrt{\frac{k}{\emptyset_e}}$$

Where k is permeability from the Kint log, and Øe is effective porosity. Øe can be obtained from Øz, the normalized porosity index, where:

$$\emptyset_{z=(\frac{\emptyset_e}{1-\emptyset_e})}$$

So the flow zone indicator formula is:

$$FZI = \frac{RQI}{\emptyset_Z}.$$

The FZI (Formation Factor Indicator) is a measure of the porosity and permeability of a formation, and is often used in the oil and gas industry to estimate fluid flow rates and reserves. The RQI (Rock Quality Index) is a measure of the strength and hardness of the rock.

Amaefule et al. (1993) proposed a graph that relates the FZI and RQI, which can be used to estimate the reservoir properties of a rock formation. The graph shows that the FZI and RQI are inversely related, and that there are several intervals of FZI values that correspond to the same unit of reservoir quality

Based on the cutoff obtained from the FZI versus RQI graph, the intervals of FZI values that correspond to the same unit of reservoir quality can be determined. This means that within each interval, the reservoir properties are considered to be similar, and can be treated as a single

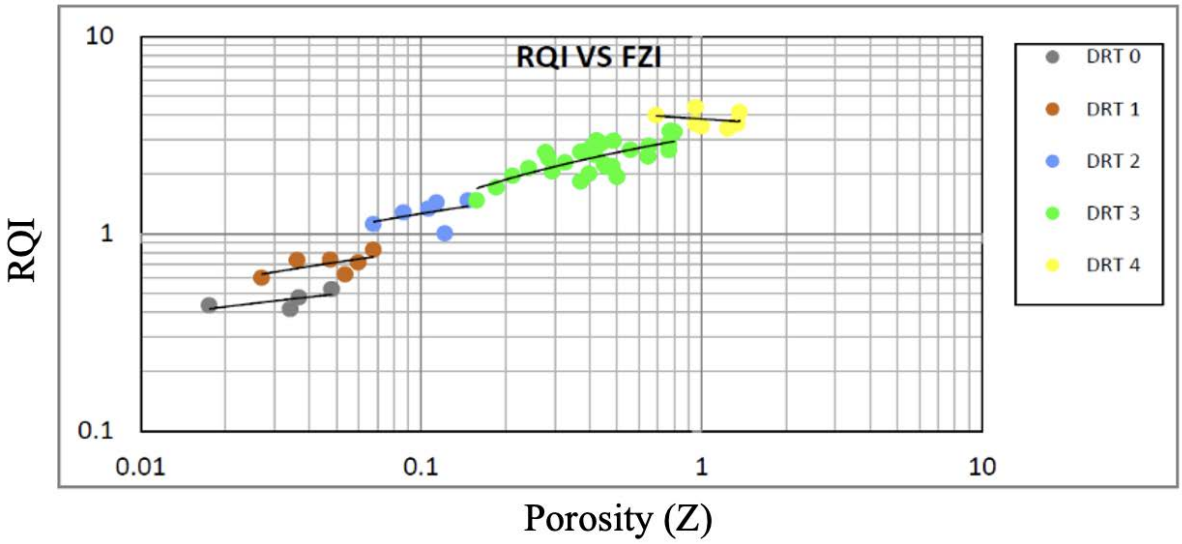

Figure 4. Correlation between RQI (Y axis) vs FZI (X axis) based on Rock Type classification

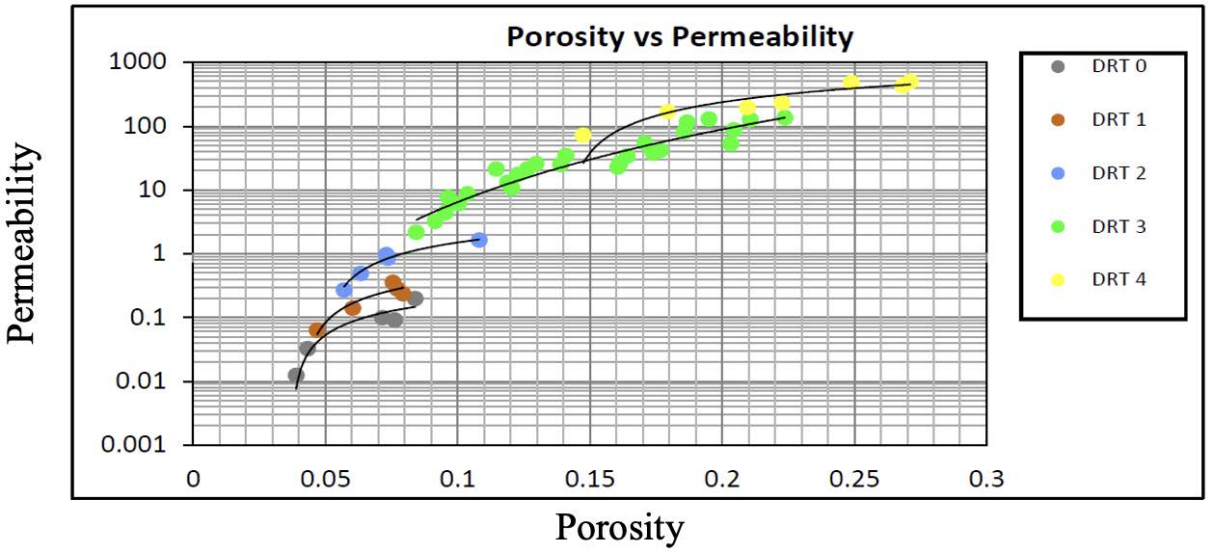

Figure 5. Correlation between porosity (X axis) and permeability (Y axis) based on RT classification

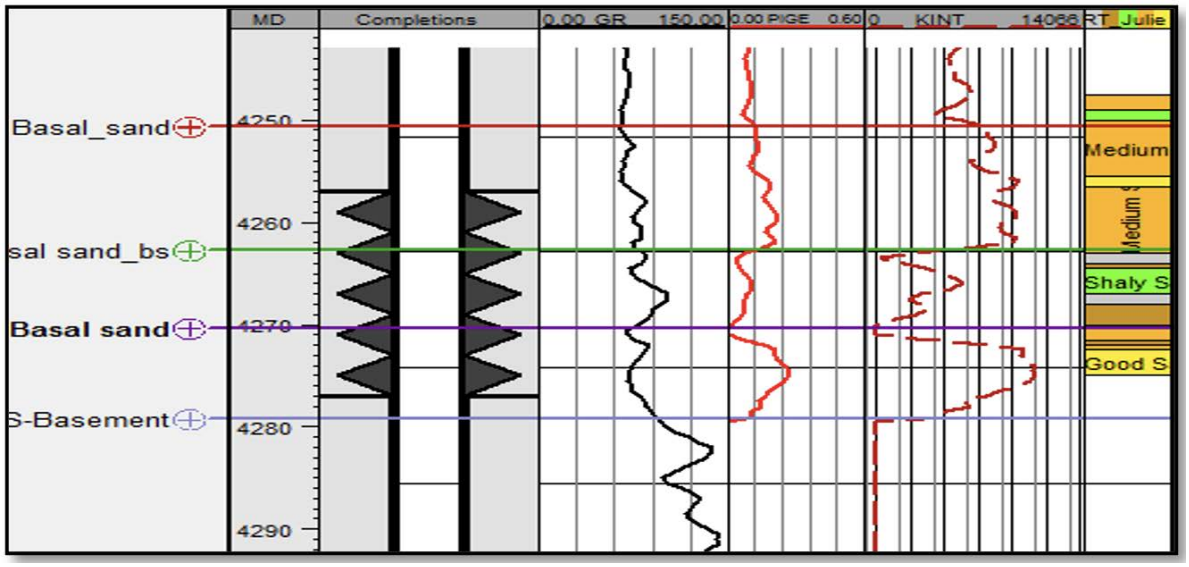

Figure 6. Correlation between porosity, permeability, RQI, and FZI based on RT classification

unit. The value of FZI is divided into several intervals, which are considered to be of the same unit based on the cutoff obtained from the FZI versus RQI graph from the A-05 well (Figure 4) and (Figure 5). Five different rock types can be classified based on the value of FZI. Different permeabilities of RT 0 to RT 4 also show the quality of each reservoir interval. The cutoff was applied to all wells in the Aryani field.

This result was used as input for the geological model. The RT method is effective enough to classify thin layers of Basal Sand. The ratio method of RQI/FZI showed a good correlation between the porosity and permeability to identify some rock types. This shows the texture of the rock has a role in distinguishing some rock types as shown in (Figure 6).

Data Analysis

Model-based inversion is one way to see the distribution of the reservoir. A feasibility study was undertaken on well A-05, showing that the crossover of AI (Acoustic Impedance) and SI (Shear Impedance) successfully separates the Basal Sand in log resolution. From the generated AI map, the Basal Sand distribution does not give a more detailed trend compared with the previous interpretation and has a poor correlation with the sand presence already known from the well data. Further analysis using the elastic properties, such as an AVO analysis and the Lame parameter, Lambda–Rho (LR), and Mu–Rho (MR), is necessary (Gray and Andersen, 2000).

The feasibility test on AI vs SI crossplot is shown in Figure 7. The AI map on the Basal Sand reservoir is displayed in Figure 8. The intercept (P) and Gradient (G) volumes can be derived from the gathered data (Castagna

et al., 1998). Near the basement, positive P values are shown in red, while negative G values are shown in blue. The results of P*G in negative values displayed in blue. Results of cross plot P vs G volume indicated by the yellow colour which indicates the distribution of Basal reservoir, indicating a similar pattern to alluvial fan deposition patterns in the NW–SE trend. These attributes are used as inputs for the geological model. The P-reflectivity (Rp) and S-reflectivity (Rs) data can also be derived from seismic data. LR and MR can be obtained by

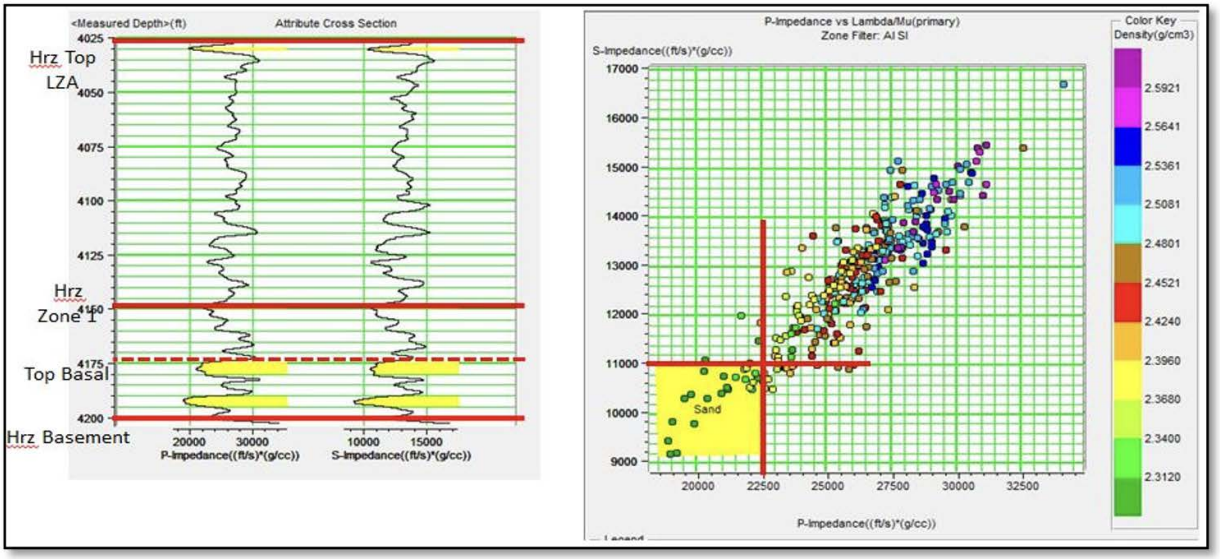

Figure 7. Feasibility test on AI vs SI crossplot

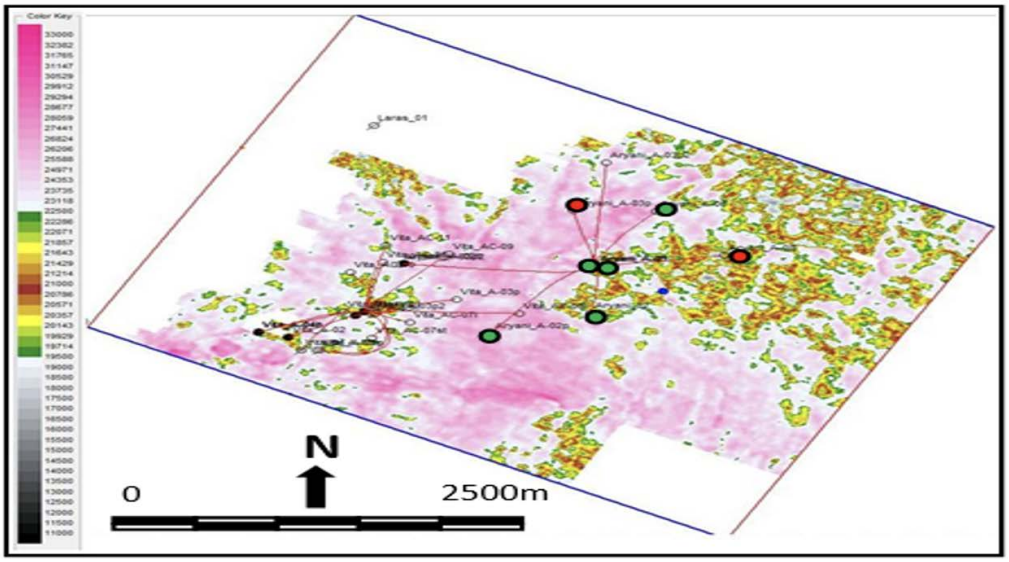

Figure 8. AI map on Basal Sand reservoir

Sand. P vs G volume is shown in (Figure 9).

The P-reflectivity (Rp) and S-reflectivity (Rs) data can also be derived from seismic data. LR and MR can be obtained by performing an AVO inversion on Rp and Rs. The cross-plot result from LR and MR from the A-05 well successfully separates the Basal Sand, with an LR cut-off ranging from 15–24 GPa*g/cc and an MR from 7.5–12.5 GPa*g/cc.

The LR section and the LR map demonstrate a good match with the well data, while the MR result is not sensitive and visibly does not match with well data. The LR map shows the lateral distribution of the Basal Sand doing an AVO inversion on Rp and Rs. The cross-plot result from LR and MR from the A-05 well successfully separates the Basal Sand, with an LR cut-off from 15–24 GPa*g/cc and an MR from 7.5–12.5 GPa*g/cc.

The LR section and the LR map show a good match with the well data, while the MR result is not sensitive and visibly does not match with well data. The LR map shows the lateral distribution of the Basal Sand reservoir similar to alluvial fan deposition patterns in the NW–SE trend. These processes are shown in Figure 10 (Intercept & Gradient Volume), Figure 11 (Feasibility test on Lambda-Rho and Mu-Rho), Figure 12 (Lambda-Rho section) and

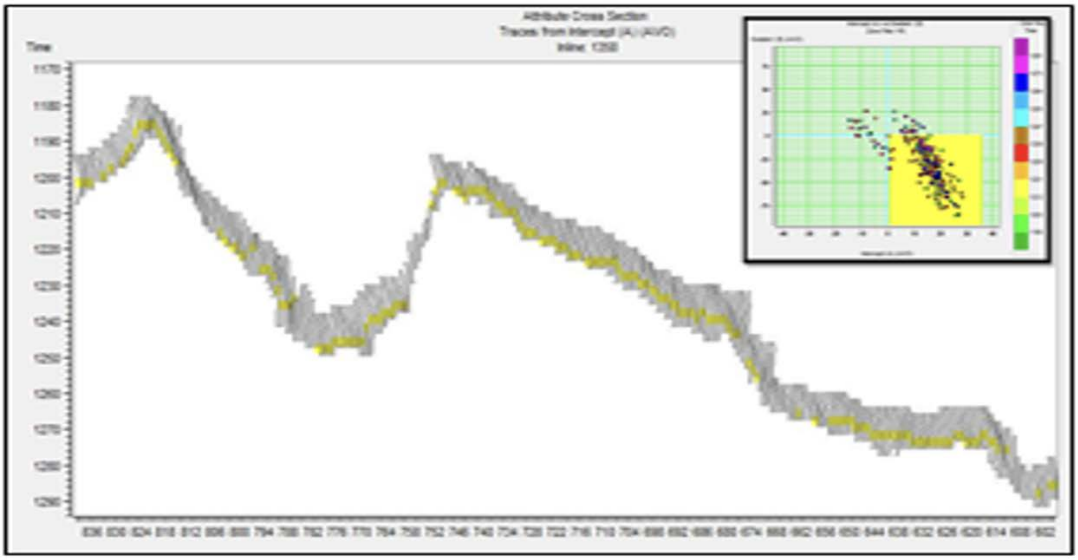

Figure 9. P vs G volume indicated by yellow colour

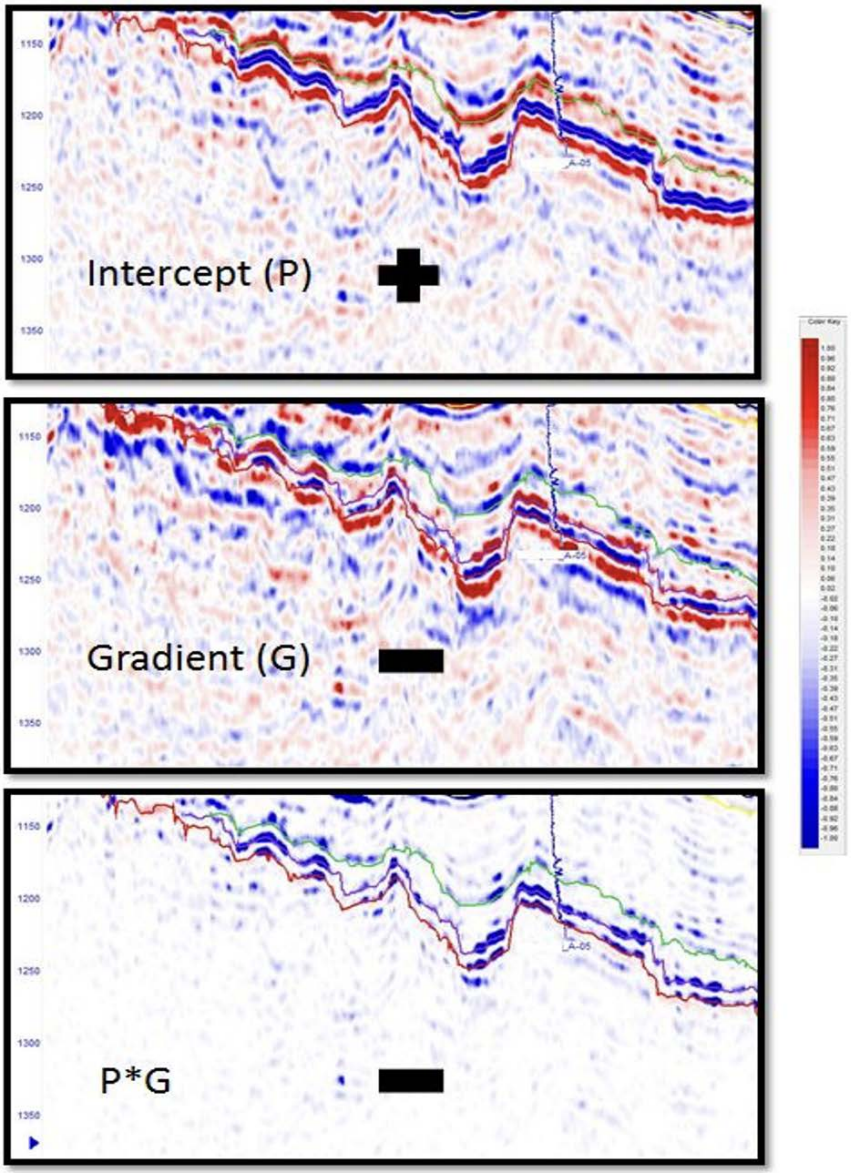

Figure 9. Intercept volume (top) shows (+) near the Basement, Gradient volume (mid) shows (-), and P*G (bottom) shows (-)

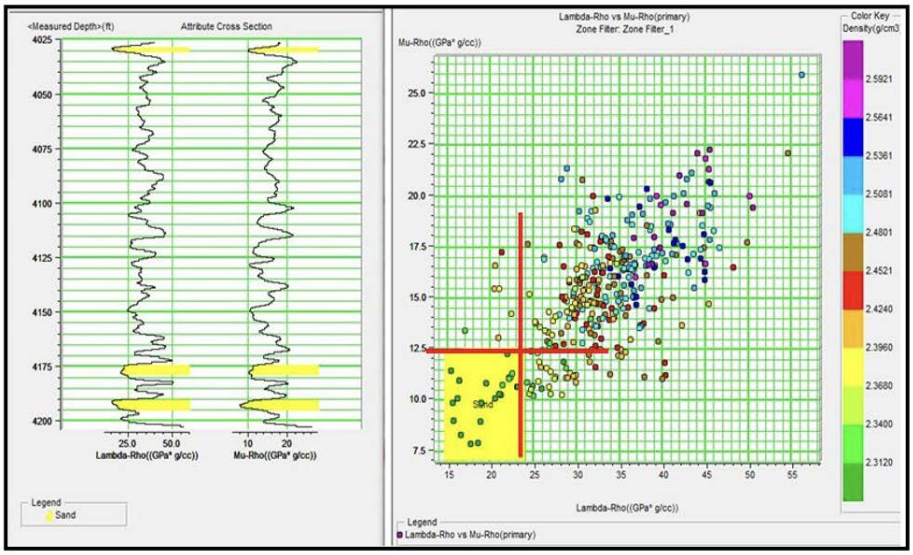

Figure 11. Feasibility test on Lambda-Rho and Mu-Rho

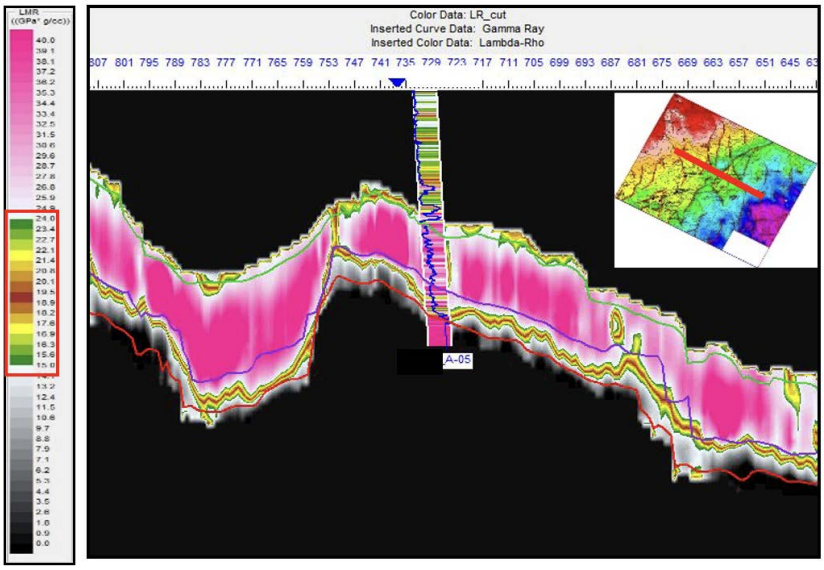

Figure 12. Lambda-Rho section that crosses on A-05 well with cut off 15-24 GPa*g/cc

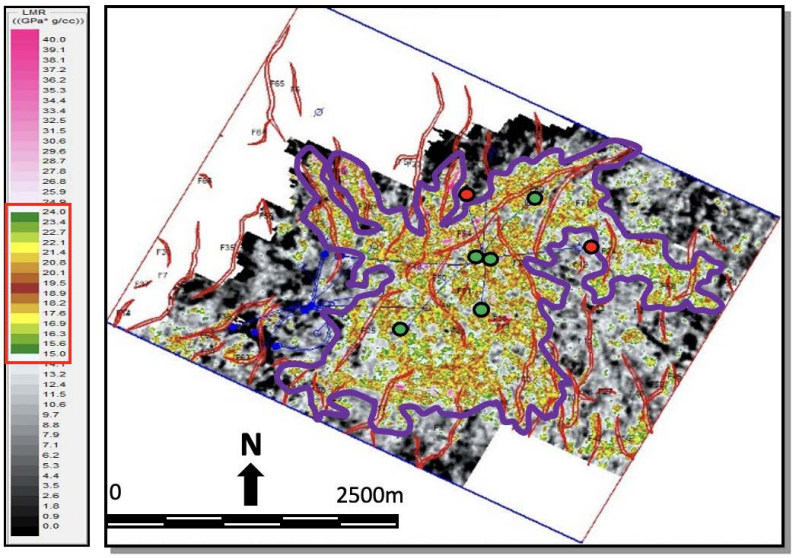

Figure 13. Lambda-Rho map shows the lateral distribution similar to alluvial fan patern

Figure 13 (Lambda-Rho map), which shows the lateral distribution similar to an alluvial fan pattern. These results were obtained from attributes that were used and utilized as an input for the geological model.

RESULTS

The four main components for constructing a static model are the seismically derived depth horizon, the fault model, layer thickness isochores, and correlated well tops. The basement horizon is the only depth horizon derived from seismic data, and other horizons are interpolated using thickness isochores. Eighteen faults are used to generate the fault model and fault segments. The facies model shown in (Figure 14) follows the conceptual depositional model for an alluvial fan system environment. Braided Channel deposits are associated with this model. Prior to facies modelling, various trends were prepared to geologically constrain the model. Data analysis of the vertical distribution of reservoir facies illustrated a common trend for most zones, where the proportion of sand generally increases towards the top of the zones. This distinct coarsening upward pattern was considered in the modelling of the reservoir facies. The total volume of clean sandstone distributed in the facies models is vertically controlled by the coarsening upward trends observed in the blocked wells. And the lateral distribution and direction of fan lobe and channels are controlled by the seismic attributes.

The distributed volume of debris-flow and mud-flow deposits is controlled by the proportions seen in the wells. It is a conceptual schematic depositional model covering the Aryani field directions within the reservoir area. It is interpreted as an alluvial fan depositional environment with both fluvial and debris flow deposits. The delineation distribution of the fan lobe follows the trend of seismic attributes.

The volume of effective porosity and permeability (Figure 15) was stochastically co-simulated with a bias towards the facies model. Each facies has its own petrophysical range, trends, and data distribution, as observed in the statistical data analysis of the upscaled well data and reflected in the model volume. Histograms, scatterplots, and data transforms were generated and analyzed for quality control of effective porosity and permeability plots. The distribution of volumes of effective porosity and permeability was compared with the stochastic output parameters to ensure consistency. Stochastic (Gaussian) conditional simulation was chosen

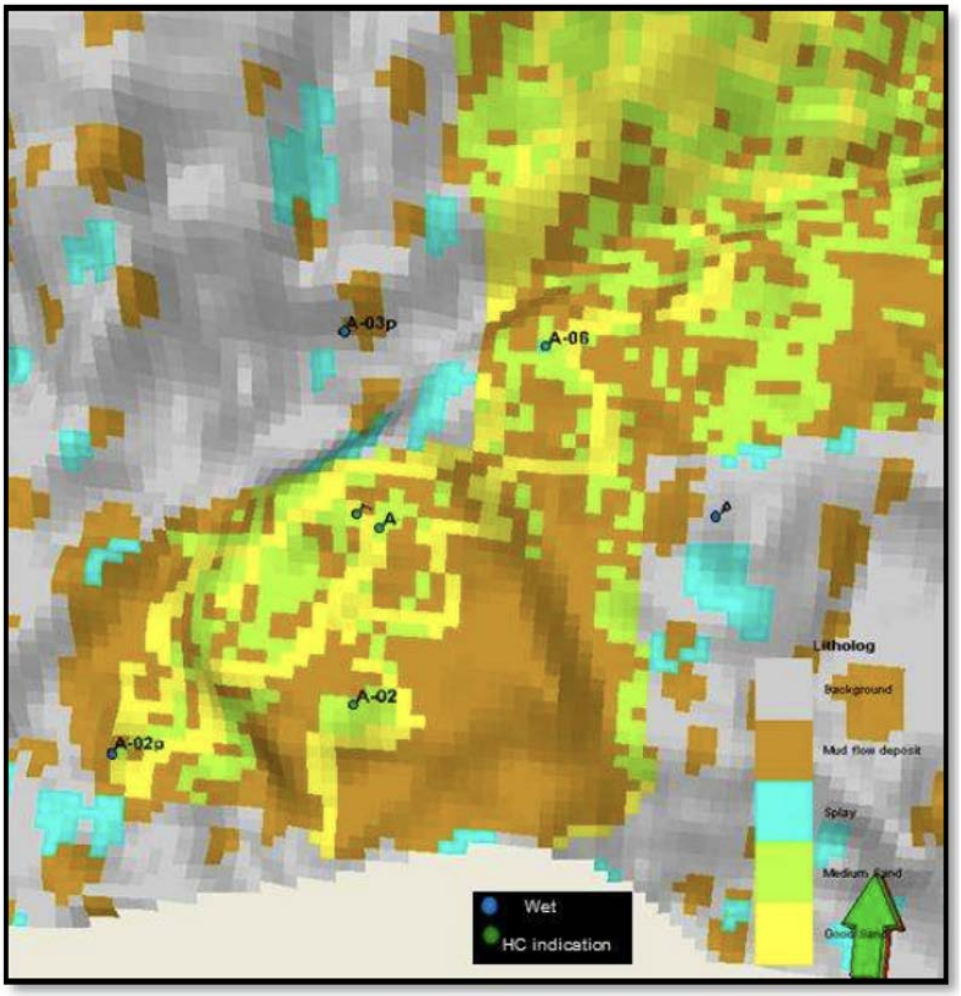

Figure 14. Facies model of Alluvial Fan deposit

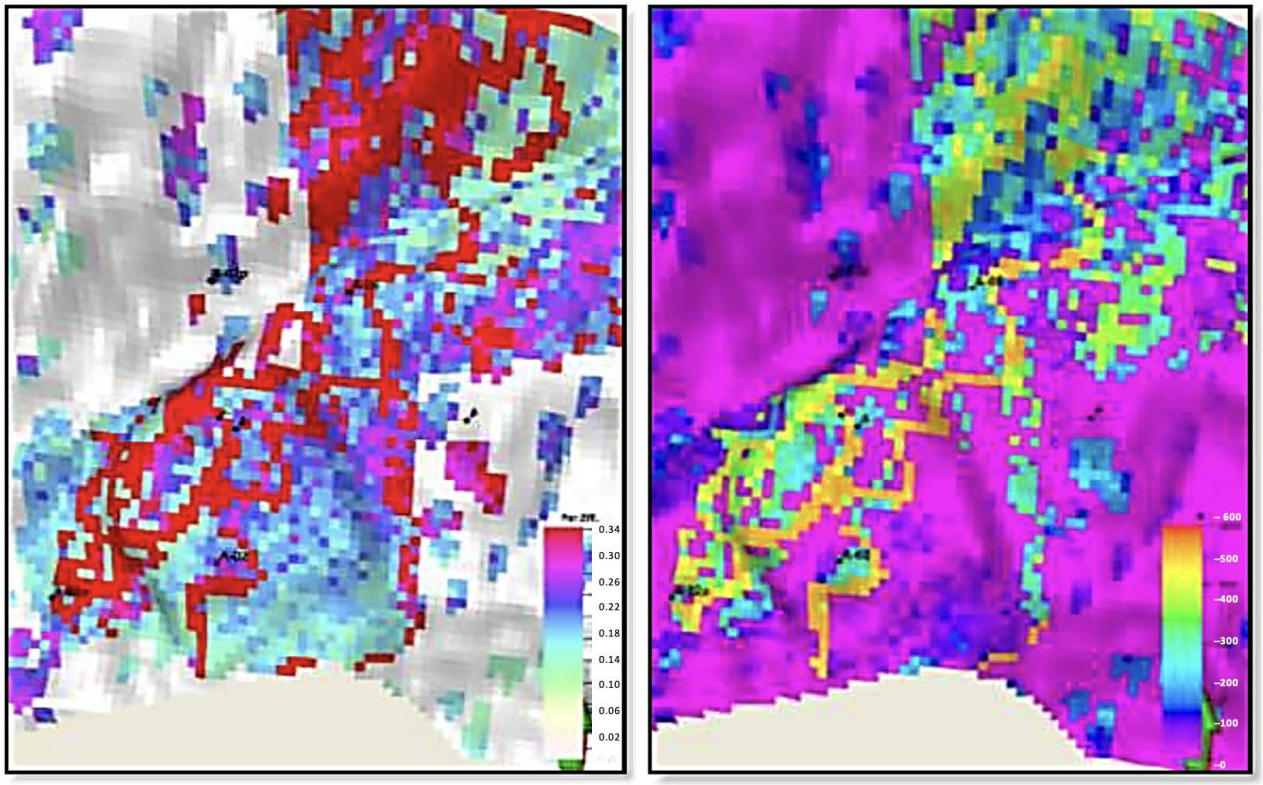

Figure 15. Porosity model (left) and permeability model (right) of Alluvial Fan deposit in Aryani Field of Widuri Area

to model the petrophysical attributes. In conjunction with the estimated variogram model, the petrophysical input parameter attributes (conditioned 100% to wells) were distributed throughout the model volume.

DISCUSSION

Based on the type of rock in the alluvial fan sediments, the interpreted Rock Type 2, which was average permeability and porosity values, is low, ranging between 6–8% and 0.1–2 mD respectively. Rock Type 3 is interpreted as mud-flow deposition and has an average permeability value of 42 mD and a porosity of 15% , indicating small channel sediment. Rock Type 4, which has a relatively high permeability average of about 280 mD and a porosity of 22%, is interpreted as the main sediment channel.

Due to the intermittent deposition process, the deposition of alluvial fans is generally not one single body but consists of several overlapping layers of sand. It is seen in the alternation of RT 0-4 which is sometimes very thin in some wells. A conceptual model of alluvial fans shows the details of the three-dimensional (3D) geometry depending on the extent of tectonic activity and the rate and volume of sediment being deposited by the streams. As indicated, alluvial fans are not generally formed as a single body but are built up over time as overlapping deposits. This is also shown in the vertical distribution of Rock Types, where the four rock types repeatedly overlap each other.

The results of the core data analysis from the A-05 well as a key well indicate that the depositional environment developing in the Aryani field is an alluvial fan as shown in Figure 16. It contains a wide range of grain sizes and many angular rock fragments. This reflects the fact that the sediments have not been transported very far from their source before being deposited. The nearest high topography is located in the northern area, and toward the south, down fan direction, the mean grain size of the sediment rapidly decreases. Alluvial fans contain a large amount of debris-flow and mud-flow deposits, leading to abrupt and erratic changes in facies, both laterally and vertically.

Alluvial fan deposits are not the result of steady deposition. Rather, a series of sporadic events, representing the discharge of an intermittent stream system is the major process. Nilsen (1982), subdivided alluvial fan deposits into two basic types. The first type consists of stream-flow deposits, which result from intermittent streams flowing in poorly defined, braided channels over the surface of the fan. Stream-flow deposits are usually coarse-grained, well sorted and stratified, with much of the clay matrix washed out. The second type consists of debris-flow and mud-flow deposits in which a saturated mass of material, often consisting of larger rocks supported in a mud-rich matrix, moves as a sediment gravity flow down the surface of the fan. As a whole, the fan body is formed through a complex interlaying of these basic types of sediment. A 3D schematic of the alluvial fan environment is shown in Figure 17.

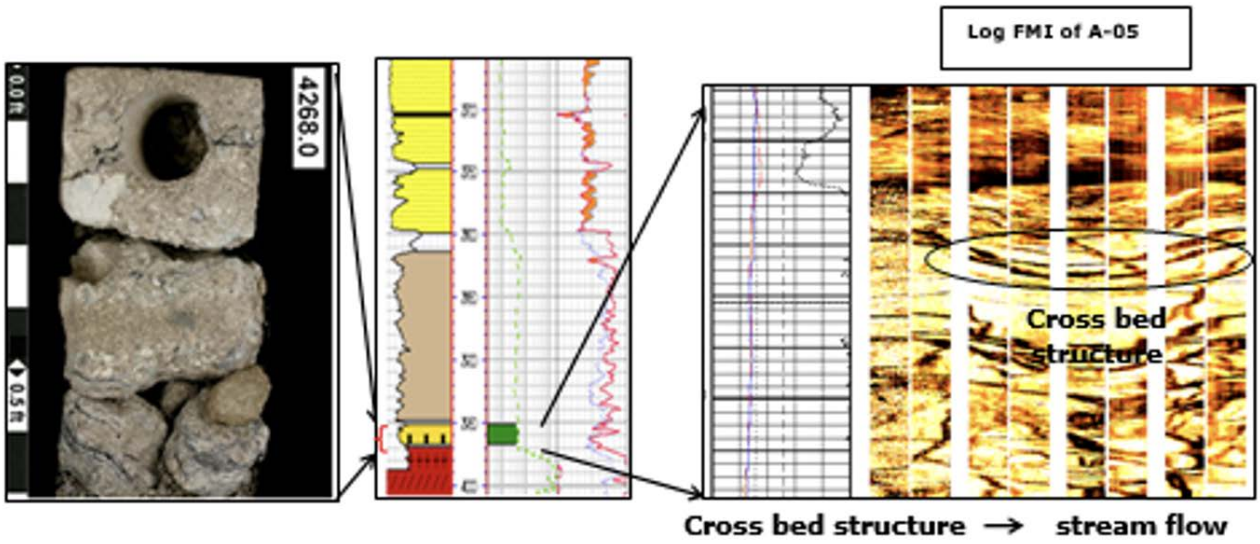

Figure 16. Core data and well logs indicate Basal Sand deposited in the Mid-Fan

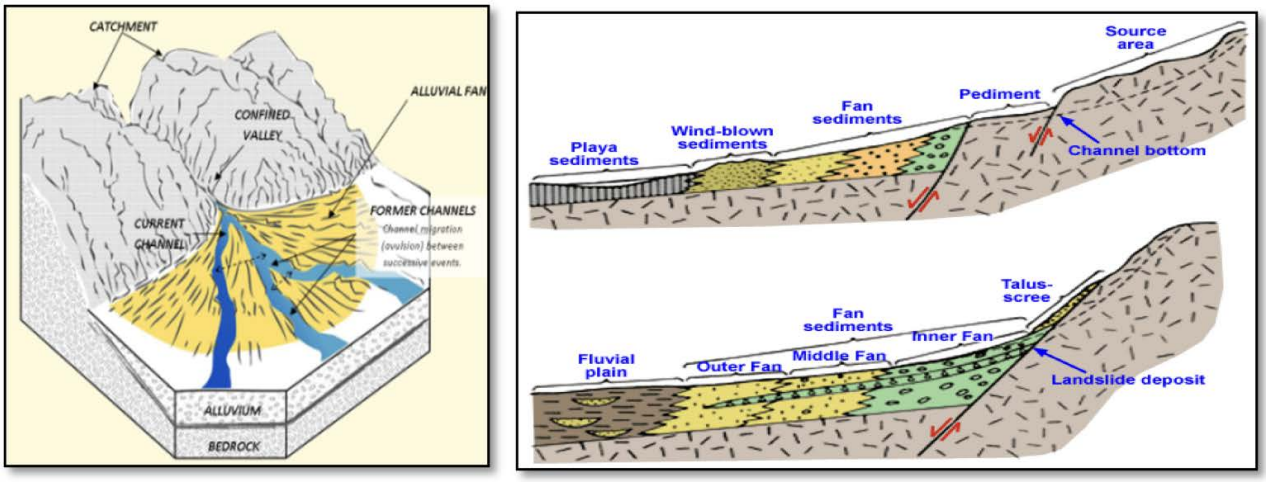

Figure 17. 3D schematic of Alluvial Fan environment (Nilsen, 1982)

CONCLUSIONS

From this research, the boundary of the Lower Zelda member geometry has defined an NW–SE trend but for the Basal Sand distribution, there is still an inconsistency between the well data and the isochrones maps. An integrated geophysical and geological analysis has been conducted for Basal Sand reservoir characterization. A low resistivity reservoir of Oligo-Miocene Talangakar Formation Basal Sand reservoir in the Aryani field of Widuri Area in Asri Basin has distinctive characteristics that require integration analysis to identify the distribution of alluvial fan sediments. By analyzing elastic properties such as Lambda Mu Rho, the lateral distribution of a thin Basal Sand reservoir has been resolved, revealing as an alluvial fan deposition pattern.

Geocellular modelling is done, using a combination of modelling methods, Truncated Gaussian for geological conditions which have lithological boundaries that are quite firm (hard boundary) and Object Model for the transition boundary (soft boundary). Rock Type and seismic attribute methods have proven to be effective in classifying thin layers of Basal Sand. The ratio method of RQI/ FZI showed a good correlation between porosity and permeability to identify different rock types. This shows the significance of rock texture in distinguishing various rock types.

ACKNOWLEDGEMENTS

The authors would like to thank the management of Pertamina Hulu Energi OSES, Pertamina EP, Pertamina Sub-holding Upstream (PHE), and SKK MIGAS, for their permission to publish this paper. Thank you to all Geosciences & Reservoir Team of the Subsurface Development Planning Department - PHE OSES, Talangakar Formation Technical Interests Group, all lecturers and civitas academica of Post-Graduate Program, Faculty of Geological Engineering, Universitas Padjadjaran for sharing beneficial, fruitful, and constructive discussions during this research and manuscript preparation.

REFERENCES

Aldrich, J.B., Pinehart, G.P., Ridwan, S., and Schuepbach, M.A., 1995. Paleogene Basin Architecture of the Sunda and Asri Basins and Associated Non-Marine Sequence Stratigraphy, *Proceedings of International Symposium on Sequence Stratigraphy, Indonesian Petroleum Association*, Jakarta, May 1995, 261-287.

Aki, K., and Richards, P.G., 1980. *Quantitative Seismology: Theory and Methods*, Vol 1, W.H. Freeman and Co.

Amaefule, J.O., Altunbay, M., Tiab, D., Kersey, D.G., and Keelan, D.K., 1993. *Enhanced Reservoir Description - Using Core and Log Data to Identify Hydraulic (Flow) Units and Predict Permeability in Un-cored Intervals/Wells,* Society of Petroleum Engineers 26436.

Castagna, J.P., Swan, H.W., and Foster, D.J., 1998. Framework for AVO Gradient and Intercept Interpretation, *Geophysics,* 63, p948-956.

Gray, F.D., and Andersen, E.A., 2000. The Application of AVO and Inversion to Formation Properties, *World Oil,* Vol. 221, No. 7.

Guo, G., Diaz, M.A., Paz, F., Smalley, J., and Waninger, E.A., 2007. Rock Typing as an Effective Tool for Permeability and Water-Saturation Modeling: A Case Study in a Clastic Reservoir in the Oriente Basin. *SPE Res Eval & Eng* 10 (6): 730-739. SPE-97033-PA.

Nilsen, T.H., 1982. Alluvial fan deposits. In Scholle, P.A. and Spearing, P. (eds.), Sandstone Depositional Environments. *Memoir: American Association of Petroleum Geologists* 31: pp. 49–86.

Ralanarko, D., Syafri, I., Abdurrokhim, and Nur, A.A., 2020. Seismic Expression of Paleogene Talangakar Formation, Asri & Sunda Basins, Java Sea, *Indonesian Journal of Sedimentary Geology,* ISSN 0853-9413, No. 46, 21-43.

Ralanarko, D., Syafri, I., Abdurrokhim, and Nur, A.A., 2021. A Success Case of Widuri Area Rejuvenation, Asri Basin, Offshore SE Sumatra Block, Indonesia, *Bulletin of Marine Geology*, DOI: http://dx.doi.org/10.32693/bomg.36.2.2021.704

Ralanarko, D., Ramadhan, M.I., Fauzielly, L., Winantris, Syafri, I., and Abdurrokhim, 2021. Facies Association and Paleogeography Reconstruction pada at Transition Zone Talangakar Formation, Asri Basin, Offshore Southeast Sumatra, Indonesia, *Journal of Marine Geology*, DOI: http://dx.doi.org/10.32693/jgk.19.2.2021.736

Smith, G., and Gidlow, P. M., 1987. Weighted Stacking for Rock Property Estimation and Detection of Gas: *Geophys. Prosp.,* 35, 993–1014.

Wight, A., Friestad, H., Anderson, I., Wicaksono, P., and Remington, C.H., 1997. Exploration History of the Offshore Southeast Sumatra PSC, Java Sea, Indonesia, in: Petroleum Geology of Southeast Asia, Fraser, Matthews, and Murphy (eds.), *Geological Society Special. Publication* No. 126, p. 121-142.

Young, R. and Atkinson, C.D., 1993. A Review of Talangakar Formation (Oligo-Miocene) Reservoirs in the Offshore Areas of Southeast Sumatra and Northwest Java. Clastic Core Workshop, *Spec. Publication of the Indonesian Petroleum Association*, 177-210.